

3D distribution of YSOs in Orion A with *Gaia* DR2

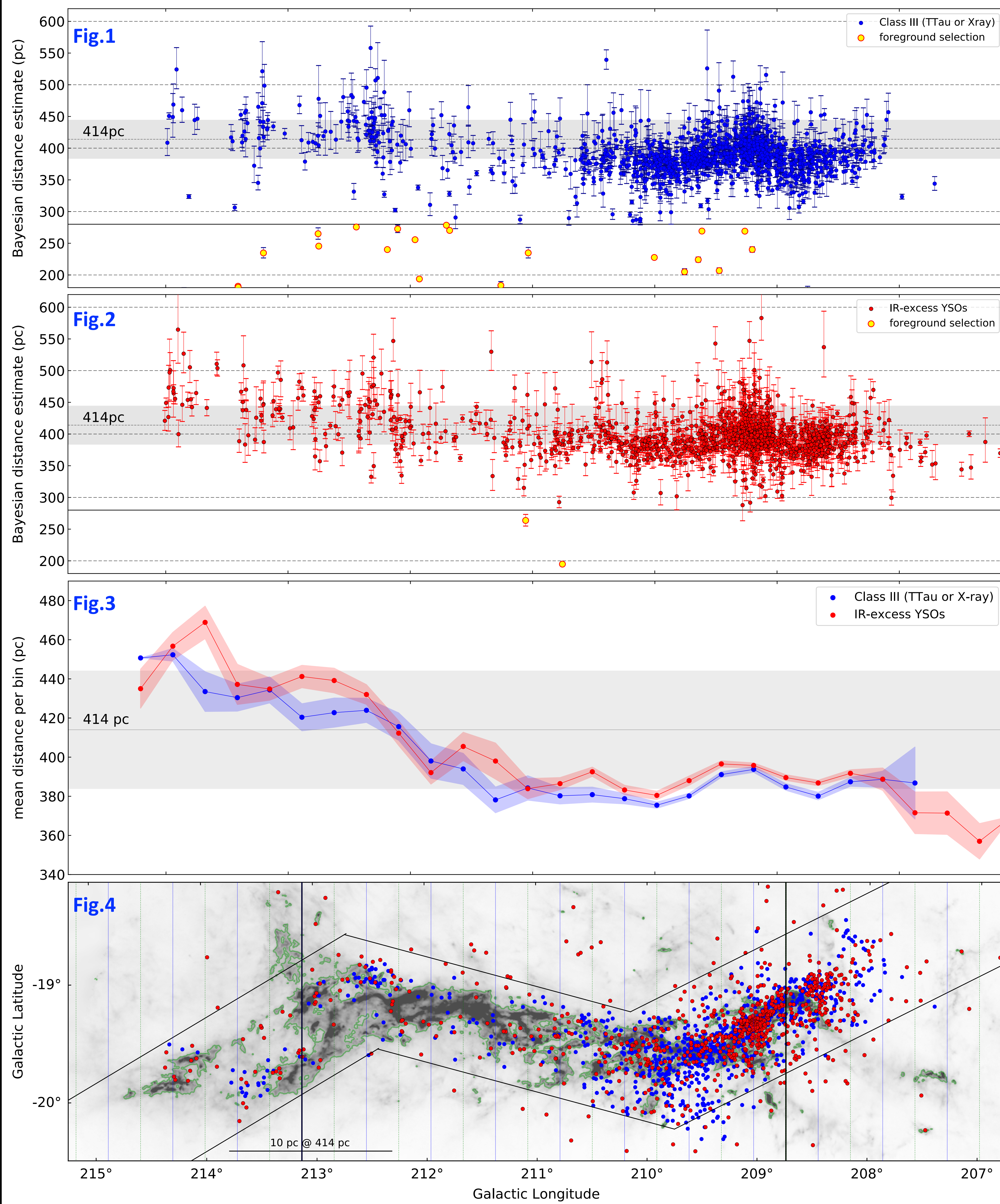
An informed view on Star Formation Rates & Efficiencies



Josefa Grossschedl¹, João Alves¹, Stefan Meingast¹, Charles Lada², Álvaro Hacar³, Christine Ackerl¹, +Vienna Gaia Team¹
 University of Vienna¹, CFA², Leiden University³

josefa.elisabeth.grossschedl@univie.ac.at

(a) YSO distance distribution along the cloud



Figs. 1. to 4. We use bayesian distance estimates [1] to get the mean distances per 4pc-wide bin (Fig.3) with the blue/red shaded areas showing the standard error of the mean. We apply the following cuts on the *Gaia* DR2 data before averaging: (1) $280\text{pc} < \text{distance} < 600\text{pc}$, (2) $(\text{parallax_err}/\text{parallax} < 0.1) \& (\text{astrometric_sigma5d_max} < 0.5\text{mas}) \& [(\text{astrometric_excess_noise} < 1\text{mas}) \mid (\text{astrometric_excess_noise} > 1\text{mas}) \& (\text{astrometric_excess_noise_sig} < 2)]$. The grey shaded area in Figs. 1 to 3 shows the assumed distance to Orion A at $414 \pm 30\text{pc}$.
Fig. 4. Planck-Herschel-Extinction dust-column density map [10]. The green contour outlines the star-forming denser parts of the cloud at $A_V > 0.8\text{mag}$ [9]. The vertical blue/green lines show the 4pc bins (at 414pc, factor 2 over-sampled). Note: Class III sources appear less scattered in 2D due to pointed surveys (X-ray and emission-line) while Class IIs were selected in the whole presented VISTA region.

(b) SFR and SFE along the cloud

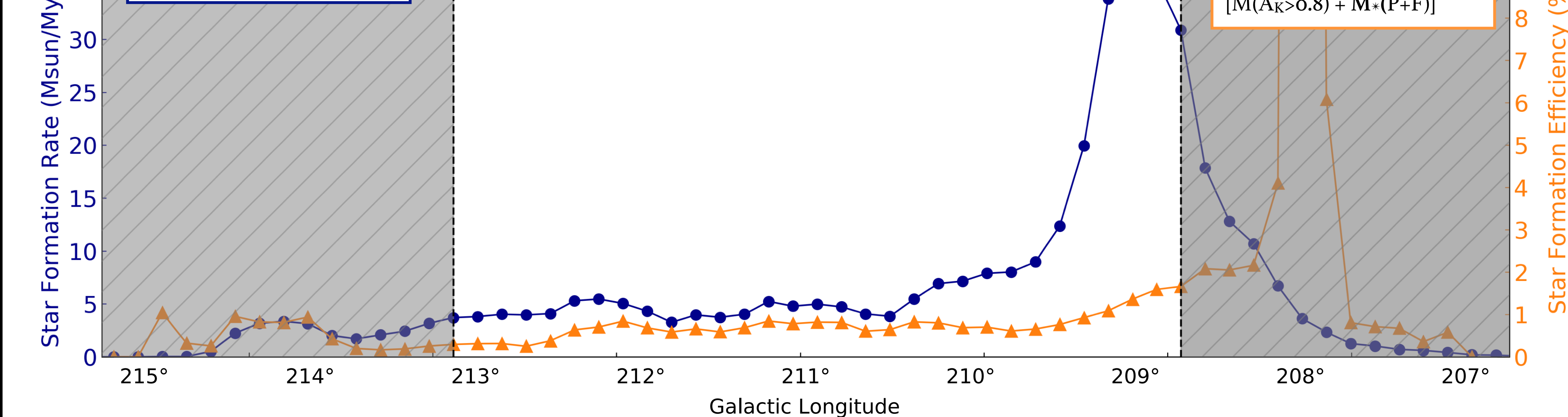


Fig. 7. SFR and instantaneous iSFE along l (same x-axis as Fig. 4), again estimated in vertical 4pc bins (factor 4 over-sampled). The star-forming cloud mass is calculated using the green extinction threshold at $A_V > 0.8\text{mag}$ [9]. The SFR is calculated including all known YSOs with IR-excess (~3000) while the iSFE is calculated by using only the younger protostars and flat-spectrum sources (P+F~350), since these are likely still projected near their birth-sites in the cloud. The grey shaded areas indicate the cloud boundaries, excluding regions without significant gas mass, and can be ignored.

Takeaway Points

- ★ The GMC Orion A is inclined $\sim 68^\circ$ along the line-of-sight
- ★ Class II and III sources show a similar distribution on average, with Class IIIs lying slightly in-front
- ★ What causes the "bump" at the ONC?
- ★ SFE is about constant across the cloud while the SFR shows variations factor of ~ 10

Introduction

The giant molecular cloud Orion A is the closest massive star forming region to earth ($\sim 414\text{pc}$ [13]) and therefore a prime location to study the laws of star formation. Using a deep NIR ESO-VISTA survey [13], we refined existing YSO catalogs [3,11] and added about 200 new candidates, leading to a sample of ~ 3000 YSOs with infrared-excess [7]. Together with *Gaia* DR2 [4], we are able to (a) investigate the 3D distribution of young stars across the cloud and (b) construct resolved maps of star formation rate and efficiency.

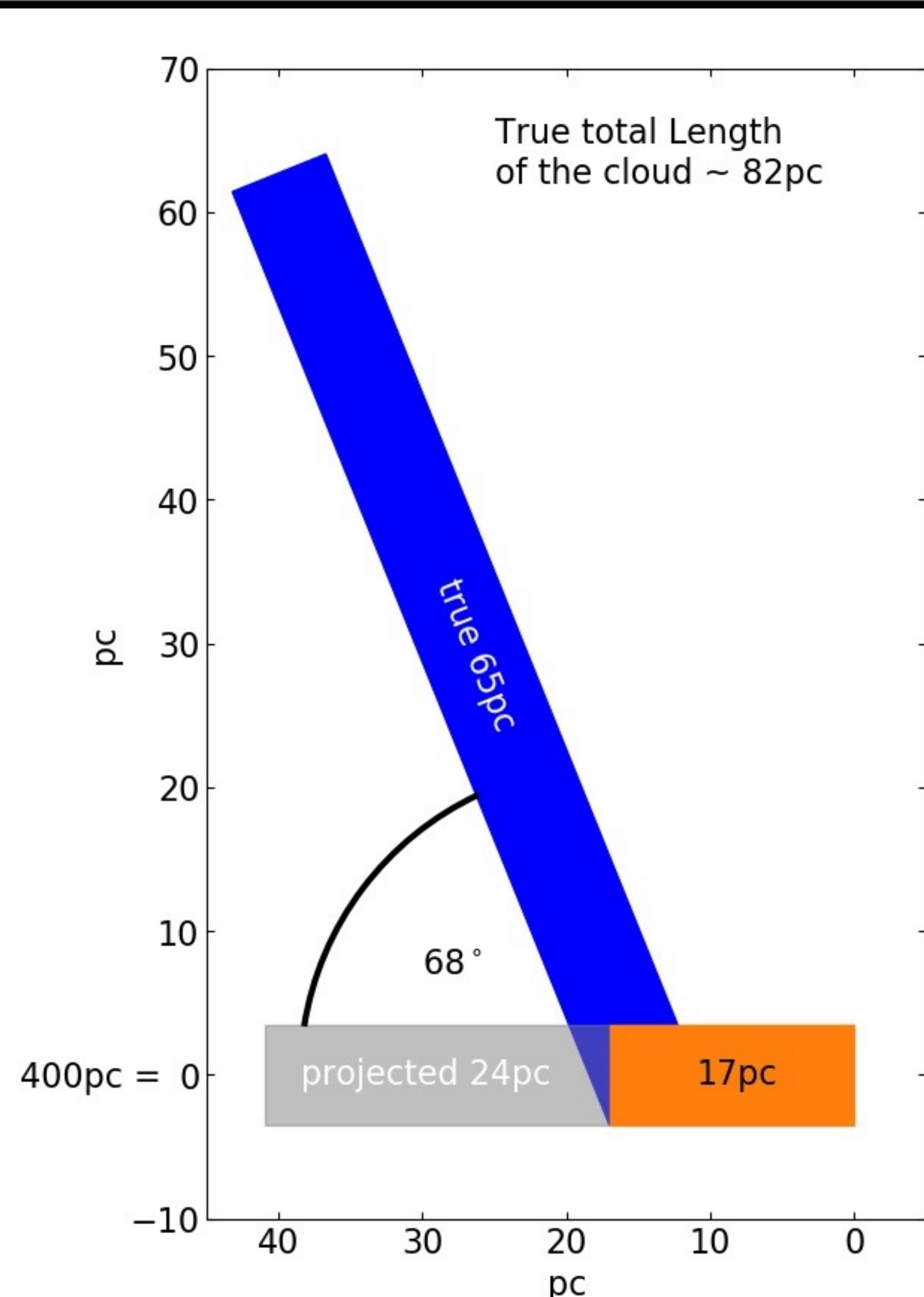


Fig. 5

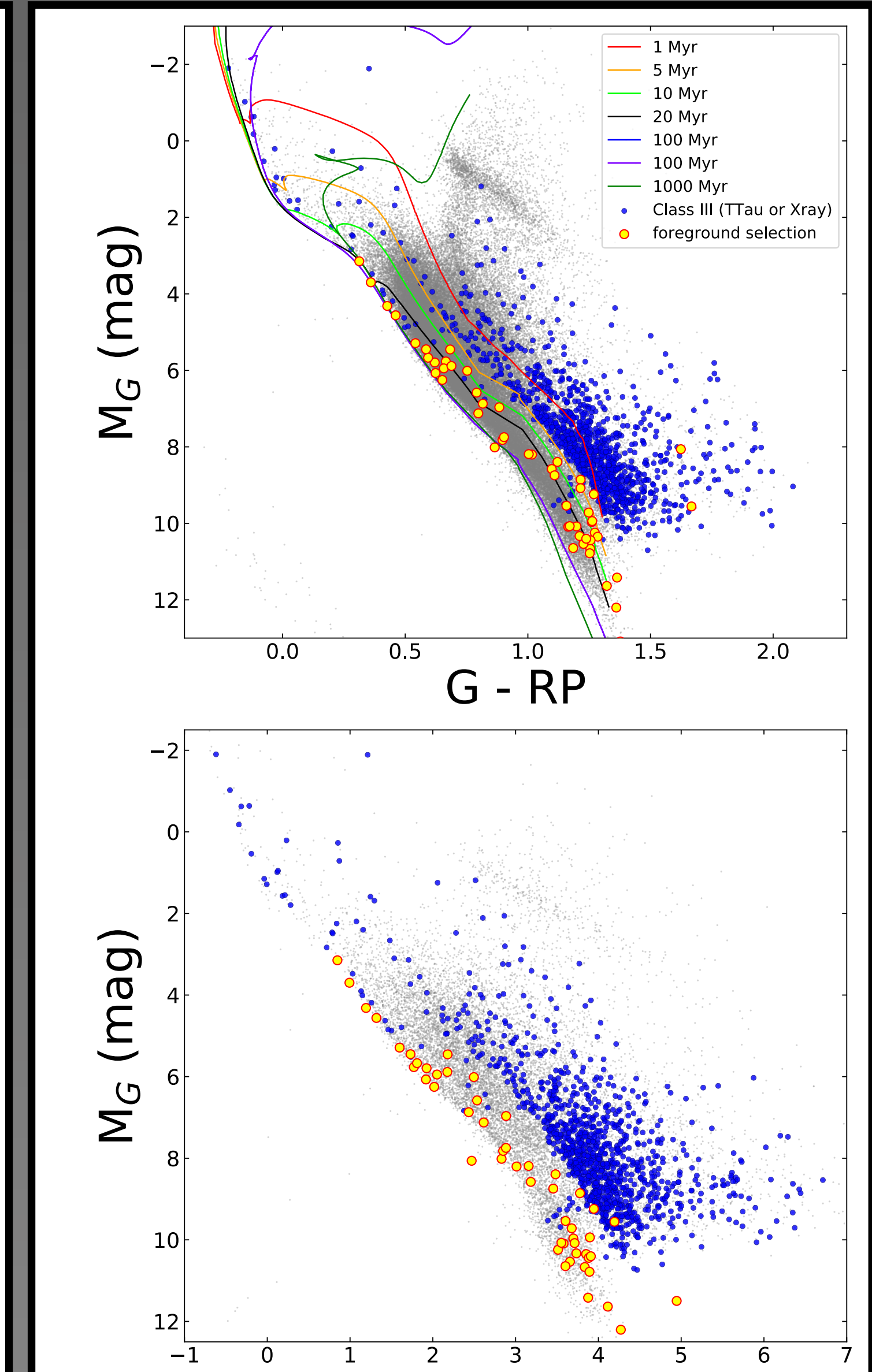


Fig. 6

Fig. 6. Two examples of observed HR-Diagrams using *Gaia* DR2 and VISTA-Ks photometry. Grey dots are all sources towards Orion A, with Class III sources over-plotted in blue. The yellow sources are identical to the selected foreground from Fig. 1. They nicely follow a separate, more evolved sequence as compared to the majority of Class IIIs, which appear younger than 5 Myr (using PARSEC Isochrones [11], $Z=0.0152$).

(a) *Gaia* DR2 results

We present *Gaia* DR2 results for ~ 900 Class III candidates (selected with X-rays [5,6,15,16] or as T-Tauri stars [2,8,17]) and ~ 1000 mid-infrared-selected YSOs in OrionA (mostly ClassII). We use the positions of these YSOs to infer on the 3D structure of the cloud (distance and inclination), and the relation between the different YSO populations (Class III and II). **Figures 1 & 2** show the distance distribution along l of Class IIIs (blue) and IIs (red), respectively. To estimate the mean distance along the cloud (Fig.3), we split the region into evenly-sized 4pc-wide bins, shown in Fig.4, and we use only sources projected near the cloud (within the black borders).

The trend of Class IIs in Fig.3 indicates, that the head of the cloud ($208.5^\circ < l < 211^\circ$), including the ONC, appears to be on the plane of the sky at about 400pc (extent $\sim 17\text{pc}$), while the tail (L1641), surprisingly, appears to be inclined along the line of sight ($\sim 68^\circ$), from about 400pc at $l=211^\circ$ to about 460pc at $l=214.5^\circ$. This is shown schematically in Fig.5. The Class III sources follow overall a similar trend, seemingly lying slightly in-front of the Class IIs (on average ~ 5 to 10pc). This suggests an age gradient towards the location of the sun.

As another interesting result, we find that the two clusterings at the tail are likely more distant (420pc to 450pc) than estimated with X-ray luminosities (250pc to 280pc [16]). Moreover, the "bump" at the ONC is striking, and its cause is not yet clear (2 mixed populations, erroneous data near the nebula, less extinction due to excavated area).

(b) SFR & SFE in Orion A

In a similar manner, we study the star formation rate (SFR) and instantaneous efficiency (iSFE) across the entire OrionA GMC, using the whole YSO sample of ~ 3000 sources and the Planck-Herschel-Extinction map from Fig.4 to estimate the gas mass. The variation of the two parameters along l is shown in Fig.7, taking into account distance variations to calculate the dense cloud mass (no significant difference to const. cloud mass).

We find that the SFR varies by a factor of ~ 10 across the cloud while the iSFE is about constant (within a factor 2). The increased SFR at the head of the cloud, including the ONC, could be explained by cloud compression due to external feedback mechanisms (e.g. SNe, local massive stars). Remarkably, the efficiency of converting dense gas into stars seems to be largely independent of external processes and might be an intrinsic property of the star forming gas. As an alternative, the huge over-density of sources at the ONC might include several populations (bursts) mixed along the line of sight.

References: [1] Bailer-Jones et al. 2018 [arXiv:1804.10121]; [2] Fang et al. 2009, A&A 504, 461; Fang et al. 2013, ApJS, 207, 5; Fang et al 2017, AJ, 153, 188; [3] Furlan et al. 2016, ApJS, 224, 5; [4] Gaia Collaboration et al. 2016, 2018b; [5] Getman et al. 2005, ApJS, 160, 319 (COUP); [6] Getman et al. 2017, ApJS, 229, 28 (SFINCS); [7] Grossschedl et al. subm. at A&A; [8] Hsu et al. 2012, ApJ, 752, 59; Hsu et al. 2013, ApJ, 764, 114; [9] Lada et al. 2010, ApJ, 724, 687; [10] Lombardi et al. 2014, A&A, 568, C1; [11] Marigo et al. 2017, ApJ, 835, 77; [12] Megeath et al. 2012, AJ, 144, 192; [13] Meingast et al. 2016, A&A, 474, 515; [14] Menten et al. 2007, A&A, 474, 515; [15] Pillitteri et al. 2013, ApJ, 773, 80 (XMM-Newton, L1641); [16] Pillitteri et al. 2016, ApJ, 820, L28 (XMM-Newton, K-Ori); [17] Szegedi-Elek et al. 2013, ApJS, 208, 28

This project is funded by the Austrian Science Fund (FWF) under project number P 26718-N27